Planta (2006) 224: 472–480
DOI 10.1007/s00425-006-0223-2

ORIGINAL ARTICLE

Takehiko Shimada · Ryohei Nakano
Vladimir Shulaev · Avi Sadka · Eduardo Blumwald

Vacuolar citrate/H^+ symporter of citrus juice cells

Received: 14 December 2005 / Accepted: 29 December 2005 / Published online: 27 January 2006

Abstract We have isolated a cDNA, designated *Citrus sinensis* citrate transporter 1 *CsCit1* encoding a novel vacuolar citrate/symporter. Immunoblots using antibodies raised against CsCit1 showed that the protein is localized to the juice sac cell vacuoles. The highest expression of *CsCit1* and the amount of protein in the juice sac cell vacuoles coincided with the developmental stage at which the vacuolar citrate content began declining with the concomitant increase in vacuolar pH. Vacuoles from *Sacharomyces cereviseae* expressing *CsCit1* displayed a citrate-dependent H^+ efflux, and our results clearly demonstrate that CsCit1 is able to mediate the electroneutral co-transport of H^+ and citrate ions, since the citrate-dependent H^+ fluxes are not affected by changing the electrical potential difference across the tonoplast. The roles of CsCit1 in mediating citrate efflux from the vacuole and on citric acid homoestasis in Citrus juice sac cells are discussed.

Keywords Acidity · Citrate · Citrus · Homeostasis · Symporter · Vacuoles

Introduction

One of the most distinctive characteristics of citrus fruits is their capacity to accumulate high levels of citric acid in their juice sacs and very low levels of other organic acids such as malate. Citric acid is not translocated form the leaves to the fruit, but it is synthesized in the juice sac cells (Ramakrishnan 1971). The citric acid synthesized in the mitochondria of the juice sac cells (Canel et al. 1996) is transported out of the mitochondria into the cell cytosol and then translocated into the vacuole. The accumulation of citric acid into the vacuole is accompanied by a large influx of protons that is mediated mainly by the vacuolar H^+-ATPase (Muller et al. 1997). This influx of protons reduces the vacuolar pH and provides a driving force for additional citrate uptake into the vacuole where citric acid acts buffering the vacuolar acidic pH (Muller and Taiz 2002). Citric acid accumulation and pH in the juice sac cell vacuoles is tightly regulated during fruit development and can vary among different cultivars, and in general, the higher the vacuolar citric acid concentration, the more acidic is the vacuolar pH (Echeverria and Burns 1989).

Different mechanisms have been described for the transport of citrate into the plant vacuole, through the operation of anion channels (Oleski et al. 1987; White and Smith 1989; Rentsch and Martinoia 1991), and through the action of ATP-dependent transporters (Canel et al. 1995). Nevertheless, the mechanisms that regulate citrate homeostasis in *Citrus* fruits are not clear. Here, we described the identification and characterization of CsCit1, a novel citrate/H^+ symporter in the juice sac cell vacuoles of Washington navel oranges. Measurements of CsCit1 activity together with its expression profiles during fruit development support the role of CsCit1 in vacuolar citrate homeostasis in *Citrus* fruits.

Materials and methods

Plant material

Navel orange (*Citrus sinensis* cv Washington) fruit at different developmental stages were obtained from the Lindcove Research and Extension Center, University of

T. Shimada and R. Nakano contributed equally to this work.

T. Shimada · R. Nakano · E. Blumwald (✉)
Department of Plant Sciences – Mail Stop 5, University of California, One Shields Ave, Davis, CA 95616, USA
E-mail: eblumwald@ucdavis.edu
Tel.: +1-530-7524640
Fax: +1-530-7522278

V. Shulaev
Virginia Bioinformatics Institute, Blacksburg, VA 24061, USA

A. Sadka
Department of Fruit Tree Species, ARO, The Volcani Center, 50250 Bet Dagan, Israel

California. Juice sac tissues were collected and used immediately for pH measurement and protein preparation or stored at −80°C for organic acids analysis and RNA extraction.

Isolation of the full-length CsCit1 cDNA and determination of the CsCit1 genomic structure

RNA was extracted from the juice sac tissues of young Navel orange (*Citrus sinensins* cv Washington) fruit by the hot borate method (Wan and Wilkins 1994), and poly (A^+) RNA was isolated using Oligotex mRNA kit (Qiagen, Valencia, CA, USA). The first-strand cDNAs, synthesized by RT from 2 μg of the poly (A^+) RNA, were used as a template for the RT-PCR using primers designed based on sequences of *AttDT* homologues in the Citrus EST database (http://www.cgf.ucdavis.edu). These primers were 5′-ttggaacattatattgcttttagg-3′ and 5′-ctgttacggagacttgattgagag-3′. The amplified 537 bp fragment was cloned into the pGEM-T Easy vector (Promega, Madison, WI, USA) and used for subsequent library screening. Plasmid cDNA libraries constructed from juice sac-tissues of young or mature fruits were kindly provided by A. M. Dandekar (Department of Plant Sciences, UC Davis, CA, USA). For the library screening, 2.0×10^6 colonies were plated, and corresponding filters were hybridized overnight at 60°C in Church buffer (Sambrook et al. 1989) with a ^{32}P-radiolabeled probe of the cDNA fragment obtained by RT-PCR (Prime-It II Random Primer Labeling Kit, Stratagene, La Jolla, CA, USA). Filters were washed at low-stringency [twice at 60°C in 2× SSC and 0.1% (w/v) SDS or 15 min] or high-stringency [twice at 60°C in 2× SSC and 0.1% (w/v) SDS for 15 min and twice at 60°C in 0.1× SSC and 0.1% (W/V) SDS for 20 min]. Positive colonies were carried through a second screening and sequenced. Genomic DNA extracted from young leaves was used as a template for PCR using primers, 5′-ctcgtatcgtgttacacgttc-3′ and 5′-ggagacttgattgagagaaacc-3′, designed within the 5′ and 3′ untranslated regions of *CsCit1* cDNA. The amplified fragment was cloned into pGEM-T Easy vector vector and sequenced. The introns and exons were determined by comparison between genomic and cDNA sequences.

Southern and Northern blot analyses

DIG-labeled cDNA probes were synthesized using a PCR DIG probe synthesis kit (Roche Applied Science, Indianapolis, IN, USA) and primers were designed to label ca. 800 bp 3′-end region of the *CsCit1*cDNA. For Southern blot analysis, a 5-μg sample of genomic DNA was digested with the restriction enzymes, *Bam*I, *Eco*RI and *Kpn*I, separated on 0.8% (w/v) agarose gel, and then blotted onto nylon membrane (Hybond-N^+, Amersham Biosciences, Piscataway, NJ, USA). The membrane was hybridized with the DIG-labeled probes in DIG Easy Hyb hybridization buffer (Roche Applied Science) at 65°C overnight. After hybridization, the membrane was washed twice at 37°C in 2× SSC and 0.1% (w/v) SDS for 15 min and twice at 65°C in 0.1× SSC and 0.1% (w/v) SDS for 15 min. The membrane was then subjected to immunological detection according to the manufacturer's instructions using CDP-star as a chemiluminescent substrate for alkaline phosphatase (Roche Applied Science). For Northern blot analysis, aliquots of total RNA (10 μg) extracted from juice sac cells of fruit at different developmental stages were separated by electrophoresis on 1% (w/v) agarose gel containing 2.2 M formaldehyde and blotted onto a nylon membrane (Hybond-N^+, Amersham Biosciences). The filter was then hybridized, washed and subjected to immunological detection as described above.

Isolation juice sac cell membranes, Western blotting analysis, pH and juice sac cell organic acid content

Tonoplast-enriched membranes from juice sacs were prepared according to Müller et. al (1997) with slight modifications. The juice sacs were ground in homogenization buffer containing 0.5 M MOPS-KOH pH 8.5, 1.5% PVPP, 7.5 mM EDTA, 2 mM DTT, 0.1 mM PMSF and 0.1% (v/v) of protease inhibitor cocktail (Sigma, St. Louis, MO, USA). Homogenates were centrifuged at 1,500*g* for 20 min and then at 12,000*g* for 20 min to eliminate cellular debris and nuclei at the first spin and to pellet mitchondria enriched fraction at the second spin. The supernatant was then subjected to ultracentrifugation at 100,000*g* for 60 min. The microsomal pellet obtained was resuspended in buffer containing 10 mM Tris–Mes pH 7.6, 10% (w/w) glycerol, 20 mM KCl, 1 mM EDTA, 2 mM DTT, 0.1 mM PMSF and 0.1% (v/v) of protease inhibitor cocktail (Sigma) and further purified on a 20, 34 and 40% sucrose step gradient. After centrifugation at 80,000*g* for 2.5 h, the 0%/20% interface containing tonoplast-enriched membranes was recovered. The membranes were diluted with buffer containing 5 mM Tris–MES pH 7.6, 10% glycerol, and 0.1% (w/w) of protease inhibitor cocktail (Sigma), sedimented at 100,000 g and resuspended in 0.4–1.0 ml of the same buffer. For assessment of subcellular localization, pellet at 12,000*g* centrifugation (mitchondria-enriched fraction), the 20%/34% interface (Golgi/ER-enriched fraction), and the 34%/40% interface (plasma membrane-enriched fraction) were also recovered, washed and resuspended in the same buffer. For the production of antibodies raised against CsCit-1, the amino acid stretch 'PALSEYLDKANLKRE' marked in Fig. 1 was synthesized with the addition of a N-terminus Cys to allow its conjugation with KLH. The KLH-conjugated peptide was immunized into two rabbits and the antibodies were affinity-purified from serum using peptide-conjugated SulfoLink gel column (Pierce, Rockford, IL, USA). Proteins prepared from juice sacs as described above and yeast as described below

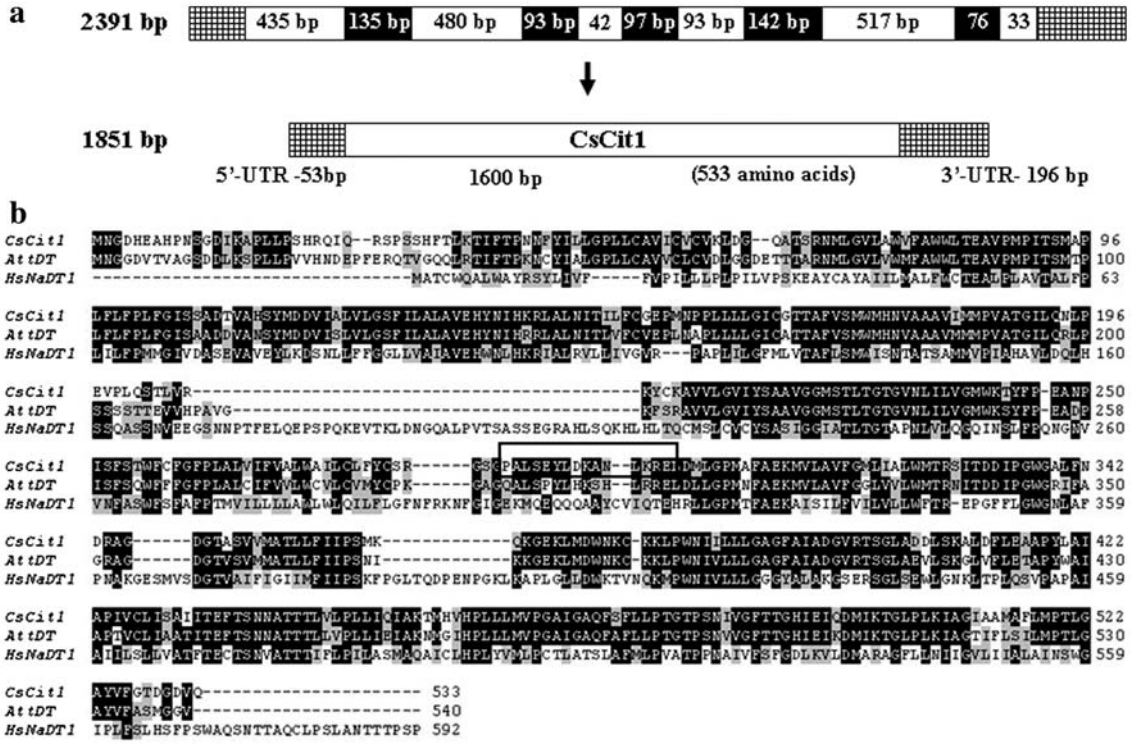

Fig. 1 Structure of *CsCit1* and amino acid sequence of CsCit1. **a** The genomic clone of *CsCit1* consist of six exons (*white boxes*) and five introns (*black boxes*). Full cDNA clone is 1,881 bp long encoding a 533 amino acids protein with a predicted molecular mass of 57.5 kDa and a pI of 6.7. **b** Amino acid sequence of CsCit1 was compared with the *Arabidopsis thaliana* decarboxylate transporter (AttDT AAN86530) and the *Homo sapiens* sodium-coupled citrate transporter (HsNaCT; CAC19843). Gaps to optimized the alignment were created using Genetyx-Win Ver.7.05 (Software Development). Identical amino acids at conserved positions are labeled by inverse print, similarity is indicated in grey. *Box in solid line* indicate the hydrophilic domain PALSEYLDKANLKRE used for the preparation of antibodies

were resolved by 10% Tris-Glycine SDS-PAGE and analyzed by Western blot analysis using the anti-CsCit1 antibodies (1:1,000) and anti-PPase (1:20,000, kindly provided by Dr. Phil Rea, University of Pennsylvania) as primary antibodies, and anti-rabbit IgG, HRP F(ab′) fragment (1:10,000, Amersham Biosciences) as secondary antibody. The blots were visualized by enhanced chemiluminescence (ECL) using Western blot detection reagents (Amersham Biosciences). The juice extracted from juice sacs was filtered through a 25 μm mesh and pH values were determined by taking direct readings on a finely calibrated pH meter (AR15, Accumet Research, Fisher Scientific, Houston, TX, USA).

Measurements of organic acids

Orange juice cell sacs at different developmental stages were lyophilized (Labconco Freezone 12 L, Kansas City, MO, USA) and stored at −80°C. A total of 10 mg of lyophilized material were transferred into 1.5 ml microfuge tubes, five replicates per size. A 750 μl aliquot of methanol and 50 μl of ribitol (50 μg ml^{-1} water stock) and two 3.2 mm chrome-steel balls (Biospec Products, Bartlesville, OK, USA) were added to each microfuge tube and pH adjusted to between 5 and 6. Each microfuge tube was then treated for three cycles of 60 s each in a Retsch mixer mill 200 (Newtown, PA, USA) and sonicated for 5 min (Branson 3510, Danbury, CT, USA). The resulting tissue slurry was transferred to 5 ml glass screw-cap vials (Sun-SRI, Duluth, GA, USA), 750 μl of water was added, and treated with a focused, high-intensity, acoustic shock-wave using a Covaris E-100 (Woburn, MA, USA). After treatment, a two ml aliquot of chloroform was added, vortexed for 1 m, extracted at 70°C for 30 m, and centrifuged at 4,800 rpm for 30 m at 4°C. The polar fractions were transferred to 1.5 ml HPLC vials and concentrated for 7 h (Labconco centrivap, Kansas City, MO, USA). After concentration, samples were methoximated with 80 μl of 20 mg ml^{-1} methoxyamine hydrochloride in pyridine for 90 min at 30°C with constant shaking and then trimethylsilylated with 80 μl of MSTFA + 1%TMCS for 30 min at 37°C. Solutions were transferred to glass inserts within the 1.5 ml HPLC vials prior to injection. Sample volumes of 1 μl were injected at a split ratio of 25:1 into a GC/MS system: A200s autosampler (Leap Technologies, Carrboro, NC, USA), a Trace GC gas chromatograph, and a Trace DSQ dual-stage quadropole mass spectrometer (Thermo Finnigan, Austin, TX, USA), manufactured in 2004. Tuning and mass

calibration was done using the reference gas tris(perfluorobutyl)amine (CF43). Chromatography was performed using a 30 m×250 μm (5 m guard) AT-5MS (Alltech Associates, Deerfield, IL, USA). Injection temperature was 230°C, the interface was 310°C, and the ion source was 200°C. Oven temperature program was 5 min at 70°C, followed by a 5°C min^{-1} ramp to 310°C, 1 min at 310°C, and a final 6 min at 70°C before the next injection. Carrier gas was helium at a constant flow of 1 ml min^{-1}. Mass spectra were recorded at 2 scans s^{-1} over 50–650 m/z. Quantitation of compounds was done using a processing method in Xcalibur v1.4. Peak area was integrated with the ICIS algorithm. Statistical analysis of peak area was done using the SAS system v9.1 (SAS Institute, Cary, NC, USA).

Expression of CsCit1 in yeast and vacuole isolation

The ORF of *CsCit1* was ligated into the p426-TEF vector (obtained from American Type Culture Collection) and transferred into *Saccharomyces cerevisiae* vacuolar protease-deficient strain MM476 (MAT α, *pep4–3, leu2, trp1, ura3–52, prb1–1122*) (kindly provided by Morris Manolson, University of Toronto). Intact vacuoles were isolated as described elsewhere (Ohsumi and Anraku 1981). To obtain citrate-loaded tonoplast vesicles, the intact vacuoles were collected at the top of the gradient and incubated in a buffer containing 20 mM Mes–Tris pH 5.0, 20 mM KCl, 200 mM potassium citrate pH 5.0 and 0.1% (v/v) of protease inhibitor cocktail for 30 min at 4°C. The vacuoles were then centrifuged at 100,000*g* for 45 min at 4°C and the tonoplast vesicles were resuspended in 20 mM Tris–MES pH 5.0 and 0.1% protease inhibitor cocktail. This method has been show to yield right-side-out vesicles with minimal contamination of inside-out-vesicles (Kakinuma et al. 1981). Protein concentrations were determined by the BioRad DC Protein Assay according to the manufacturer's instructions.

Fluorescence transport assays

The fluorescence quenching of acridine orange was used to monitor the formation and dissipation of inside-acidic pH gradients across the membranes of the tonoplast vesicles (Blumwald and Poole 1985, 1987; Blumwald et al. 1987). A preset ΔpH was obtained by mixing tonoplast vesicles (pH_i = 5.0) with a buffer solution at pH_o ranging between 7.5 and 5.0 (''pH jump''). In all the experiments, citrate- and acid-loaded tonoplast vesicles (100 μg protein) were added to 0.8 ml of buffer containing 20 mM Tris–MES buffer pH 5.0–7.5, 5 μM acridine orange, 2 mM KCl and 1 μM valinomycin. Changes in the fluorescence were monitored with a Perkin-Elmer spectrofluorimeter model LS-55 at excitation and emission wavelengths of 495 and 540 nm, respectively, and a slit width of 5 nm with a 1% transmittance filter. Initial rates were measured as the slope of the relaxation of the quench over a period of ≈ 30 s. All traces were normalized to 100% quench before quantitation. Curves were fitted to the mean values of rates at each concentration measured by using KALEIDEGRAPH (Synergy Software, Reading, PA, USA). The initial rates of dissipation of pH gradients were corrected by changes in volume and/or pH changes by subtraction of those obtained with tonoplast vesicles of yeast expressing the vector p426-TEF alone.

Results

The recent identification of *At*tDt, the *Arabidopsis thaliana* vacuolar malate carrier (Emmerlich et al. 2003) and the identification of an Citrus EST homologous to *At*tDT allowed for the identification of *Cs*Cit1, a vacuolar citrate/H^+ symporter from citrus juice cells. The *CsCit1* genomic sequence is 2,391 nucleotides long containing 6 exons and 5 introns (Fig. 1a). The cloned cDNA of *CsCit1* is 1851 bp long, with a 5′-untranslated region of 516 nucleotides, a predicted ORF of 1,600 nucleotides, and a 3′-untranslated region of 429 nucleotides. The predicted ORF encodes a protein of 533 amino acids with a calculated molecular mass of 57.47 kDa. CsCit1 is predicted to contain 12 transmembrane domains and the protein displays high similarity to the *Arabidopsis thaliana* vacuolar malate/H^+ transporter AttDT (Emmerlich et al. 2003) (76.2 and 85.2% similarity and identity, respectively) and a lower similarity to the human sodium dicarboxylate cotransporter *Hs*NaDC1 (Pajor 1996) (32.8 and 52% identity and similarity, respectively) (Fig. 1b). However, CsCit1 does not display a significant similarity to known mitochondrial citrate transporters (Miyake et al. 2002) (not shown).

Immunoblots of membrane fractions form Washington navel orange juice cell sacs were used to assess the subcellular localization of CsCit1. Antibodies raised against a hydrophilic portion of CsCit1 (Fig. 1b) detected two proteins of approximately 52.4 and 46.9 kDA in the tonoplast-enriched membrane fractions (Fig. 2a). The enrichment of the fractions with tonoplast membranes was assessed using antibodies raised against the vacuolar H^+-PPiase (Fig. 2b). No noticeable cross-reactivity was observed in mitochondria-, plasma membrane- and Golgi/ER-enriched fractions of orange juiced sac cells, indicating that CsCit1 is localized to the juice sac cell vacuole. The apparent molecular mass of these bands is somewhat lower than that predicted by the amino acid sequence of CsCit1 and may reflect anomalous migration of the protein in the SDS-PAGE gel (Apse et al. 1999) or specific cleavage or degradation. In contrast, when *CsCit1* was expressed in *S. cerevisiae* and intact vacuoles and tonoplast membranes and vacuolar soluble fractions (obtained by the disruption of the intact vacuoles) were immunobloted and tested with the antibodies raised against CsCit1, only one band was

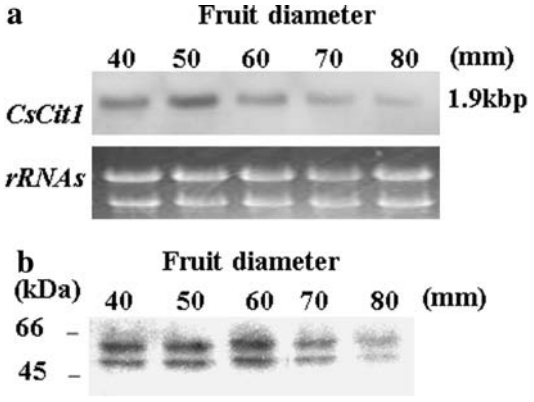

Fig. 2 Subcellular localization of CsCit1. **a** Membrane fractions were isolated from juice sac cells from fruits (60 mm diameter) on sucrose step gradients. Equal amount of protein were loaded onto onto a 10% SDS-polyacrylamide gel that was electroblotted onto a nitrocellulose membrane. Polyclonal antibodies, raised against CsCit1, were used for the immunoblot at a dilution of (1:1,000), which was developed using chemiluminescence. The lane numbers correspond as follows: (*1*) mitochondria-enriched fraction; (*2*) tonoplast-enriched fraction; (*3*) Golgi/ER-enriched fraction; (*4*) plasma membrane-enriched fraction. **b** The same electroblotted membrane incubated with antibodies raised against the vacuolar H^+-PPiase (1:2,000 dilution). **c** Purified vacuoles, tonoplast membranes or vacuolar soluble fractions from yeast expressing *CsCit1* or p426-TEF vector alone were resolved on 10% SDS-PAGE and immunobloted. Intact vacuoles (*1*), tonoplast (*3*) and vacuolar soluble proteins (*5*) from yeast expressing CsCit1; intact vacuoles (*2*), tonoplast (*4*) and vacuolar soluble proteins (*6*) from yeast expressing p426-TEF alone. Equal amount of protein (5 μg) was loaded. Polyclonal antibodies, raised against CsCit1, were used for the immunoblot at a dilution of (1:1,000), which was developed using chemiluminescence. Figures are representative of three independent experiments

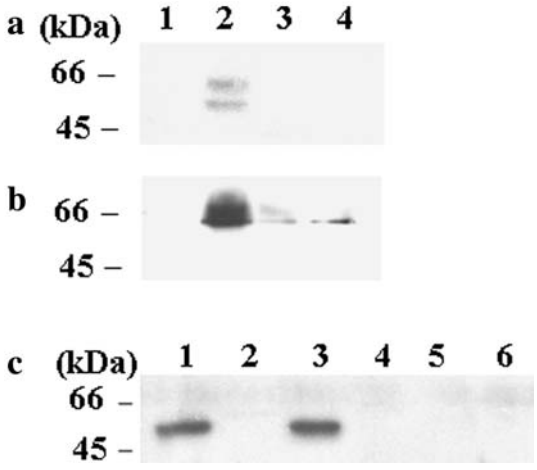

Fig. 3 Northern and Western blot analyses of CsCit1. **a** Northern blot of RNA (10 μg) isolated from juice sac tissue at different stages of development. RNA was probed with a Dig-labeled probe as described in Materials and methods. *CsCit1* transcript (1.9 kb) was detected. Apparent molecular size (kb) of the transcript is indicated to the left. Loading control is shown by EtBr staining of 35S rRNA bands. **b** CsCit1 abundance in juice sac cells tonoplast membranes. Equal amounts of protein (5 μg) were load were loaded onto a 10% SDS-polyacrylamide gel that was electroblotted onto a nitrocellulose membrane. Polyclonal antibodies, raised against CsCit1, were used for the immunoblot at a dilution of (1:1,000). Figures are representative of four independent experiments

detected. Our results clearly showed that CsCit1 localized at the yeast vacuolar membrane (Fig. 2c) and no immunoreaction was detected in tonoplasts from yeast expressing the vector alone. Preliminary results indicated that the appearance of two immunoreactive bands in tonoplast from juice sac cells was not due to the glycosylation of CsCit1 (results not shown), and whether the presence of two immunoreactive proteins at the tonoplast represents post-translational modifications of CsCit1 remains unclear.

Southern blot analysis showed that *CsCit1* exists as a single copy in the Washington navel orange genome (data not shown). In order to determine *CsCit1* expression in orange fruits, we performed Northern blot analysis of RNA isolated from juice cell sacs obtained from orange fruits at different stages of development (Fig. 3a). *CsCit1* RNA was more abundant in fruits at early stage of development (40–50 mm diameter) and decreased progressively with fruit development (fruit diameter >60 mm). Immunoblots of tonoplast-enriched fractions isolated from the same tissues (Fig. 3b) showed that the CsCit1 content of the citrus tonoplast correlated well with *Cscit1* RNA abundance, with the amounts of CsCit1 decreasing during fruit development.

The accumulation of organic acids in the juice cell vacuoles of citrus fruits is a developmentally regulated process and can vary among different varieties (Ting and Vines 1966). Although some variation exists between different varieties, citric acid is the main organic acid accumulated in the juice sac cells (Ting and Vines 1966). The analysis of organic acids content in Washington navel oranges revealed that citric acid constituted more than 95% of the organic acids in the juice cells, with exception of small fruits (less than 30 mm diameter) where quinic acid and malic acid represented 40 and 30% of the total organic acids accumulated in the fruit, respectively (Fig. 4a). The acidity of the juice cells also changed during the development of the fruit, and was inversely correlated with the juice sac cell citrate content, i.e., lower pH values with high citrate content and vice versa (Fig. 4b).

In order to measure H^+-coupled vacuolar citrate transport we isolated intact vacuoles from yeast expressing *CsCit1*. It should be noted that our attempts to perform transport assays with tonoplast vesicles from orange juice sac cells were hampered by the leakiness (non-specific high H^+ conductance) of the vesicles (results not shown). Intact vacuoles from yeast expressing *CsCit1* and vector alone were isolated and tonoplast vesicles loaded with acidic pH and citrate were obtained as described in Experimental Procedures. We avoided the loading of the tonoplast vesicles with buffers at pH $= 4.0$ or lower because under these conditions the tonoplast vesicles aggregated and were leaky (results not shown). The dissipation of an acidic-inside pH gradient in tonoplast vesicles in response to outwardly oriented citrate gradients was followed by monitoring the fluorescence quenching of acridine orange (Blumwald and

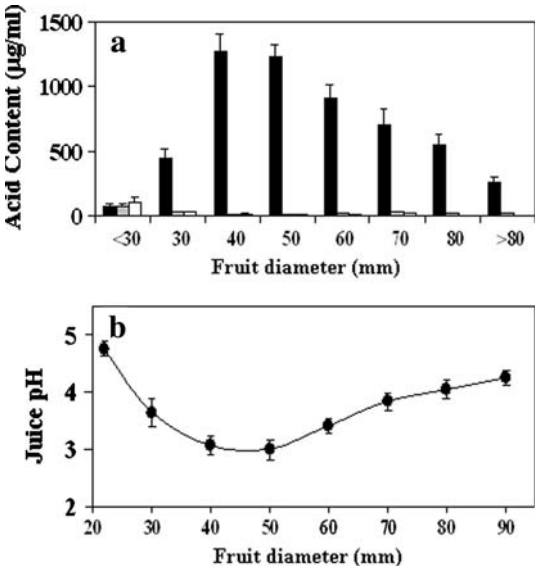

Fig. 4 Changes of organic acid content and pH in orange juice cell sacs during fruit development. **a** Relative organic acid content of Washington Navel fruits were determined in juice cell sacs at different developmental stages by LC-MS using Ribitol as an internal standard. Citrate (*solid bars*), Malate (*grey bars*), Quinate (*white bars*). Results are the Mean ± SE ($n=4$). **b** Juice cell pH. Values are the Mean ± SE ($n=5$)

Poole 1985). To generate outwardly directed citrate gradients, vesicles loaded with 200 mM K-citrate at pH 5.0 were diluted 200-fold in citrate-free medium at pH values ranging from 7.5 to 5.0 (“pH jumps”) (Blumwald and Poole 1985, 1987). Dilution of the citrate-loaded vesicles resulted in quenching of acridine orange fluorescence, and the quenched fluorescence was restored upon the addition of K^+ ions and nigericin (a K^+/H^+ ionophore) that collapsed the established pH gradient across the tonoplast vesicles (Fig. 5a,b). In tonoplast vesicles isolated from yeast expressing vector alone, the pH gradient generated by the “pH jump” was stable and only dissipated upon the addition of K^+/nigericin (Fig. 5a). On the other hand, the pH gradient established by the pH jumps in vesicles expressing CsCit1 dissipated progressively, indicating a citrate-dependent H^+ movement (Fig. 5b). The rate of citrate-dependent H^+ transport increased with the pH gradient established (Fig. 5c). Similar rates were observed when the vesicles were loaded with 200 mM citrate at $pH_i = 5.5$ and the vesicles diluted in citrate free medium with pH ranging between 8.0 and 5.5 (results not shown). The citrate-dependent H^+ efflux was diminished by the addition of 2 mM citrate and completely abolished by 20 mM citrate further indicating that CsCit1 is a citrate transporter. The rates of citrate dependent H^+-transport were obtained in the presence of 2 mM K^+ and 1 µM of valinomycin (a K^+ ionophore) in the dilution medium (Fig. 5), and similar results were obtained in the absence of K^+/valinomycin in the dilution buffer or in the presence of 5 mM K^+ and valinomycin (results not shown). Since the presence of K^+ at both sides of the membrane and valinomycin would diminish the electrical potential difference across the membrane, our results indicated that the co-transport of citrate and H^+ catalyzed by CsCit1 was electroneutral, i.e., either citrateH_2^-/1 H^+ or citrateH^{2-}/2 H^+.

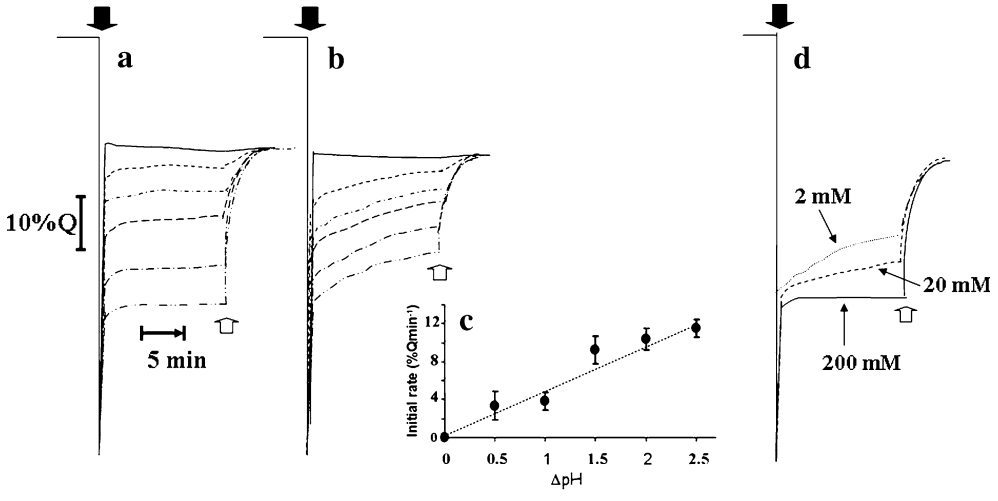

Fig. 5 CsCit1 is a citrate/2H^+ vacuolar symporter. The formation and dissipation of inside-acidic pH gradients across the membranes of the tonoplast vesicles. At the indicated times (*solid arrows*) citrate- and acid-loaded tonoplast vesicles ($pH_i = 5.0$) (100 µg protein) were added to a citrate-free solutions with pH_o ranging from 5.0 to 7.5 (pH jumps). All the experiments were performed in the presence of valinomycin and K^+ at both sides of the membrane. At the indicated times (*white arrows*) 50 mM K^+ and 5 µM nigericin were added resulting in the collapse of the ΔpH across the tonoplast membrane. **a** Tonoplast vesicles isolated from vacuoles expressing the expression vector p426-TEF alone; **b** tonoplast vesicles isolated from vacuoles expressing *CsCit1*; **c** net initial rates of H+-coupled citrate transport as a function of the pH difference (ΔpH) across the vacuolar membrane; values are the Mean ± SD ($n=4$). **d** Citrate transport from the vacuolar vesicles was inhibited by the addition of citrate to the cytosolic side. At the indicated times citrate- and acid-loaded tonoplast vesicles ($pH_i = 5.0$) (100 µg protein) were added to a solution containing 2, 20 or 200 mM citrate at $pH_o = 7.0$

Discussion

Several mechanisms have been postulated for the transport of citrate into the vacuole: (1) transport driven by the electrochemical gradient of H^+ ($\Delta\mu H^+$) across the vacuolar membrane and (2) transport driven by an ATP-dependent, $\Delta\mu H^+$-independent transporter. Flux analysis using radiolabeled malate and citrate, and the uptake inhibition of malate in the presence of citrate suggested that both compounds cross the tonoplast using the same transporter (Oleski et al. 1987; White and Smith 1989; Rentsch and Martinoia 1991; Emmerlich et al. 2003). Patch-clamp experiments demonstrated the presence of vacuolar inward-rectifying malate channels mediating the vacuolar uptake of malate in a number of plant species (Pantoja et al. 1992; Cerana et al. 1995; Pei et al. 1996; Pantoja and Smith 2002; Hafke et al. 2003). Antibodies raised against the vacuolar malate channel from *Kalanchoe diagremontiana* immunoreacted with a citrus vacuolar protein of similar molecular mass (Ratajczak et al. 2003) and the presence of malate inhibited the accumulation of citrate in tonoplast vesicles from acid lime juice cells (Ratajczak et al. 2003) further suggesting that either one channel mediates the transport of both compounds or that two different malate channel and citrate channels are highly similar. Recently, Hurth et al. (2005) showed that vacuolar inward-rectifying currents were mediated by the movement of malate into *Arabidopsis* vacuoles, nevertheless, these currents were blocked by citrate and the authors suggested that, at least in *Arabidopis*, the vacuolar uptake of citrate and malate could be mediated by two different transporters.

An alternative mechanism for citrate uptake in citrus vacuoles has been proposed. Canel et al. (1995) suggested that the accumulation of citrate into the vacuoles of citrus fruits was mediated by a ATP-driven mechanism. Working with tonoplast vesicles isolated from lemon fruits, Brune et al. (1998) further supported the notion of a primary active transport mechanism for citrate transport since ATP-driven uptake mediated a two-fold citrate accumulation of citrate in tonoplast vesicles in the absence of an electrochemical potential gradient of H^+. The physiological relevance of an ATP-dependent citrate transport in juice sac cells remains unclear. At a cytosolic pH of about 7.0, most of the citrate exported from the mitochondria into the cytosol would exist in the form of citrate^{3-}. Given the acidic vacuolar pH in lime (pH_{vac} = 2.0) (Echeverria and Burns 1989; Brune et al. 2002) and in oranges (pH_{vac} = 3.0–4.0) (Fig. 4) and the positive-inside electrical potential difference across the tonoplast, the electrogenic transport of citrate^{3-} into the citrus vacuole would be a thermodynamically favored process since the ΔpH could provide energy for the accumulation of 100–10,000 times citrate in the vacuole.

In *A. thaliana*, acidification of leaf discs promoted the expression of AttDT, the malate/H^+ co-transporter and this correlated with a dramatic decrease of total cellular dicarbonic acid levels. This led to the suggestion that AttDT could also be involved in malate export (Hurth et al. 2005). We assessed whether CsCit1 could operate in a symporter mode moving citrate out of the vacuole coupled to H^+ efflux. These experiments were based on the following rationale: (1) Because of the relatively alkaline cytosolic pH, citrate is almost completely dissociated to citrate^{3-} according to the following equation:

$$\text{Citrate}H_3 \overset{pKa_1=3.15}{\leftrightarrows} \text{Citrate}H_2^- \overset{pKa_2=4.77}{\leftrightarrows} \text{Citrate}H^{2-} \overset{pKa_3=6.39}{\leftrightarrows} \text{Citrate}^{3-}$$

The citrate^{3-} anions that enter the vacuole *via* the action of inward-rectifying channels (Rentsch and Martinoia 1991; Ratajczak et al. 2003) and possibly also via ATP-dependent facilitated transport (Canel et al. 1995; Brune et al. 1998; Ratajczak et al. 2003) are immediately protonated after entering the vacuole to citrateH_3, citrateH_2^- and citrateH^{2-}, and the predominant chemical forms of citrate will be determined by the overall vacuolar pH and the dissociation constants of the different citrate forms (Fig. 6a). Given the relative acidic vacuolar pH (Fig. 4b) a significant amount of citrate will exist in the forms of citrateH_2^- and citrateH^{2-} with vacuolar pH values of 3.0–4.0; (2) highest expression of *CsCit1* and the amount of CsCit1 in the tonoplast were attained when the fruits reached a diameter of 50 mm (Fig. 3). Coincidentally, at this development stage the vacuolar

a

pH	2.0	2.5	3.0	3.5	4.0	4.5	5.0	5.5
$CitH_3$	93.5	82.0	58.3	31	8.1	-	-	-
$CitH_2^-$	6.5	18	41.7	65.7	77.7	63.3	37.0	15.3
$CitH^{2-}$	-	-	-	3.3	14.2	36.7	61.0	75.1
Cit^{3-}	-	-	-	-	-	-	2	9.6

b

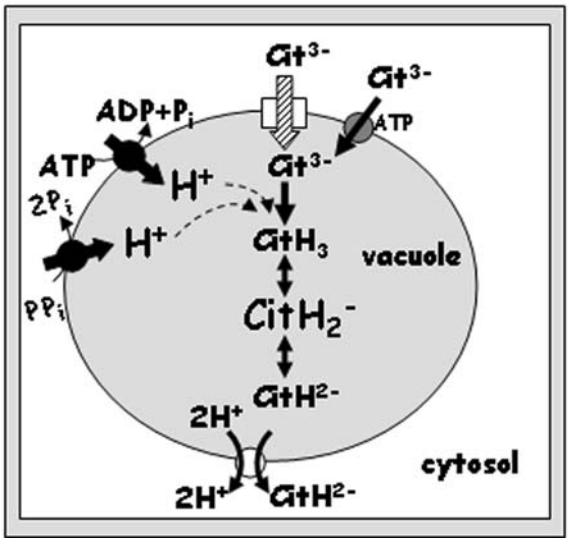

Fig. 6 Citrate homeostasis in citrus juice sac cells. **a** Citrate forms (%) as a function of vacuolar pH. Relative amounts were calculated using the Henderson–Hasselbalch relationship. **b** Diagram representing citrate homeostasis in citrus juice cells

citrate content began declining with the concomitant increase in vacuolar pH (Fig. 4), thus suggesting a possible role of CsCit1 in mediating citrate efflux into the cytosol; and (3) the electrochemical potential of H^+ across the tonoplast and the high vacuolar citrate concentrations would favor the coupled transport of citrate and H^+s out of the vacuole in a symporter mode. Our results clearly demonstrated that CsCit1 is able to mediate the electroneutral co-transport of H^+ and citrate ions, since the citrate-dependent H^+ fluxes were not affected by changing the electrical potential difference across the tonoplast (Fig. 5). Although our results could be indicative of either the cotransport of citrateH_2^-/1H^+ or citrateH^{2-}/2H^+, we believe that CsCit1 is a citrateH^{2-}/2H^+ symporter for the following reasons: (1) vacuolar pH remained below pH 3.5 without a reduction of citrate concentration, suggesting that the permeability of the citrus tonoplast for citrateH_3 and citrateH_2^- is very low, (2) vacuolar citrate concentration began to decrease at vacuolar pH values higher than 3.5, with the appearance of citrateH^{2-} in the vacuole, and (3) Although of no physiological significance, the citrate-dependent H^+ fluxes did not change when the vesicular pH_i = 5.5, a pH value at which the citrateH_2^- was significantly reduced (results not shown).

A simple model applicable to citrate transport in Washington navel orange juice sac cell vacuoles is shown in Fig. 6b. According to this model, citrate^{3-} enters the vacuole through inward-rectifying channels and possible through an ATP-dependent citrate transporter. Once in the vacuole, citrate^{3-} is rapidly protonated to citrateH_3 and citrateH_2^-. The alkalinization of the vacuole is avoided by the action of the H^+-PPiase and the H^+-ATPase that maintain the acidic-inside pH and citrateH_2^- as the main vacuolar buffer. During maturation of the fruit, the vacuolar pH increases with the concomitant increase of citrateH^{2-}, that is exported out of the vacuole by the action of CsCit1. The selectivity of CsCit1 for citrateH^{2-} and the low permeability of tonoplast for citrateH_2^- contribute to maintain the vacuolar buffer content and the acidic vacuolar pH.

Acknowledgements We thank Dr. Zhang Hui for assistance in the initial experiments. This work was supported by grant No. 5000-117 from the California Citrus Research Board, by a Research Grant No. US-3575-04R from BARD, the United States-Israel Binational Agricultural Research and Development Fund, and by the Will W. Lester Endowment, University of California.

References

Apse MP, Aharon GS, Snedden WA, Blumwald E (1999) Salt tolerance conferred by overexpression of a vacuolar Na+/H+ antiport in *Arabidopsis*. Science 285:1256–1258

Blumwald E, Poole RJ (1985) Na+/H+ antiport in isolated tonoplast vesicles from storage tissue of beta-vulgaris. Plant Physiol 78:163–167

Blumwald E, Poole RJ (1987) Salt tolerance in suspension-cultures of sugar-beet-induction of Na+/H+ antiport activity at the tonoplast by growth in salt. Plant Physiol 83:884–887

Blumwald E, Rea PA, Poole RJ (1987) Preparation of tonoplast vesicles—applications to H+-coupled secondary transport in plant vacuoles. Methods Enzymol 148:115–123

Brune A, Gonzales P, Goren R, Zehavi U, Echeverria E (1998) Citrate uptake into tonoplast vesicles from acid lime (*citrus aurantifolia*) juice cells. J Membr Biol 166:197–203

Brune A, Muller M., Taiz L., Gonzalez P., Echeverria E. (2002) Vacuolar acidification in citrus fruit: comparison between acid lime (*Citurs aurantifolia*) and sweet lime (*Citurs limmetoides*) juice cells. J Am Soc Hort Sci 127:171–177

Canel C, Bailey-Serres JN, Roose ML (1995) In vitro [^{14}C]citrate uptake by tonoplast vesicles of acidless citrus juice cells. J Am Soc Hort Sci 120:510–514

Canel C, Bailey-Serres JN, Roose ML (1996) Molecular characteriztion of the mitochondrial citrate synthase gene of an acidless pummelo. Plant Mol Biol 31:143–147

Cerana R, Giromini L, Colombo R (1995) Malate-regulated channels permeable to anions in vacuoles of *Arabidopsis thaliana*. J Plant Physiol 22:115–121

Echeverria E, Burns JK (1989) Vacuolar acid hydrolysis as a physiological mechanism for sucrose breakdown. Plant Physiol 90:530–533

Emmerlich V, Linka N, Reinhold T, Hurth MA, Traub M, Martinoia E, Neuhaus HE (2003) The plant homolog to the human sodium/dicarboxylic cotransporter is the vacuolar malate carrier. Proc Nat Acad Sci USA 100:11122–11126

Hafke JB, Hafke Y, Smith JAC, Luttge U, Thiel G (2003) Vacuolar malate uptake is mediated by an anion-selective inward rectifier. Plant J 35:116–128

Hurth MA, Suh SJ, Kretzschmar T, Geis T, Bregante M, Gambale F, Martinoia E, Neuhaus HE (2005) Impaired pH homeostasis in *Arabidopsis* lacking the vacuolar dicarboxylate transporter and analysis of carboxylic acid transport across the tonoplast. Plant Physiol 137:901–10

Kakinuma Y, Ohsumi Y, Anraku Y (1981) Properties of H^+-translocating adenosine triphosphatase in vacuolar membranes of *Saccaromyces cereviseae*. J Biol Chem 256:10859–10863

Miyake S, Yamashita T, Taniguchi M, Tamatani M, Sato K, Tohyama M (2002) Identification and characterization of a novel mitochondrial tricarboxylate carrier. Biochem Biophys Res Commun 295:463–468

Muller ML, IrkensKiesecker U, Kramer D, Taiz L (1997) Purification and reconstitution of the vacuolar H+-ATPases from lemon fruits and epicotyls. J Biol Chem 272:12762–12770

Muller ML, Taiz L (2002) Regulation of the lemmon-fruit V-ATPase by variable stoichiometry and organic acids. J Membr Biol 185:2009–220

Ohsumi Y, Anraku Y (1981) Active-transport of basic-amino-acids driven by a proton motive force in vacuolar membrane-vesicles of *Saccharomyces Cerevisiae*. J Biol Chem 256:2079–2082

Oleski N, Mahdavi P, Bennett AB (1987) Transport properties of the tomato fruit tonoplast. II. Citrate transport. Plant Physiol 84:997–1000

Pajor AM (1996) Molecular cloning and functional expression of a sodium-dicarboxylate cotransporter from human kidney. Am J Physiol Renal Physiol 39:F642–F648

Pantoja O, Gelli A, Blumwald E (1992) Characterization of vacuolar malate and K^+ channels under physiological conditions. Plant Physiol 100:1137–1141

Pantoja O, Smith JAC (2002) Sensibility of the plant vacuolar malate channel to pH, Ca^{2+} and anion-channel blockers. J Membr Biol 186: 31–42

Pei Z-M, Ward JM, Harper JF, Schroeder JI (1996) A novel chloride channel in *Vicia faba* guard cell vacuoles activated by the serine/threonine kinase, CDPK. EMBO J 15:6564–6574

Ramakrishnan CV (1971) Citric acid metabolism in the fruit tissues of *Citrus acida*. Curr Sci 21:97–100

Ratajczak R, Luttge U, Gonzalez P, Etxeberria E (2003) Malate and malate-channel antibodies inhibit electrogenic and ATP-dependent citrate transport across the tonoplast of citrus juice cells. J Plant Physiol 160:1313–1317

Rentsch D, Martinoia E (1991) Citrate transport into barley mesophyll vacuoles—comparison with malate-uptake activity. Planta 184:532–537

Sambrook J, Fritsch ER, Maniatis T (1989) Molecular cloning: a laboratory manual. Cold Spring Harbor Laboratory, vol 1, 2, 3

Ting SV, Vines HM (1966) Organic acids in the juice vesicles of Florida "Hamlin" orange and "Marsh Seedles" grapefruit. J Am Soc Hort Sci 88:291–297

Wan CY, Wilkins TA (1994) A modified hot borate method significantly enhances the yield of high-quality Rna from cotton (*Gossypium-Hirsutum* L). Anal Biochem 223:7–12

White PJ, Smith JAC (1989) Proton and anion transport at the tonoplast in Crassulacean-acid-metabolism plants: specificity of the malate-influx system in *Kalanchoe daigremontiana*. Planta 179:265–274